

**Electronic Supplementary Information (ESI)**

**Homochiral porous coordination polymers with rare utk topology and two kinds of uniform channels for enantioseparation**

Changchang Zou,<sup>a</sup> Qianqian Li,<sup>a</sup> Fujun Chen,<sup>a</sup> Haijun Wang,<sup>a</sup> Jingui Duan<sup>a,b,c\*</sup> and Wanqin Jin<sup>a\*</sup>

<sup>a</sup> State Key Laboratory of Materials-Oriented Chemical Engineering, College of Chemistry and Chemical engineering, Nanjing Tech University, Nanjing, 210009, China. Email: duanjingui@njtech.edu.cn; wqjin@njtech.edu.cn.

<sup>b</sup> Jiangsu National Synergetic Innovation Center for Advanced Materials, Nanjing Tech University, Nanjing, 210009, China

<sup>c</sup> State Key Laboratory of Coordination Chemistry, Nanjing University, Nanjing, 210023, China

## Materials and methods

All materials were of analytical grade and were used without further purification. Deionized water was used throughout. The FTIR spectra were recorded from KBr pellets in the range of 4000-500  $\text{cm}^{-1}$  on a VECTOR 22 spectrometer. The powder X-ray diffraction patterns (PXRD) measurements were carried on a Bruker axis D8 Advance 40kV, 40mA for  $\text{CuK}\alpha$  ( $\theta = 1.5418 \text{ \AA}$ ) with a scan rate of 0.2 s/deg at room temperature. Thermal analyses were performed on a TGA, STA 209 F1, NETZSCH Instruments from room temperature to 650°C with a heating rate of 10°C/min under flowing nitrogen. Luminescent spectra of the solid samples were recorded on a Hitachi 850 fluorescence spectrophotometer. The CD spectra of solid samples were recorded on J-810 Instruments by a KBr pellet spectrum of an aliquot of the powdered sample under  $\text{N}_2$  flow. Optical rotation was measured on the Autopol IV automatic polarimeter at 20 °C, 589nm in the 10cm, 2.5 ml sample cell (EtOH).

## Synthesis of ligands

*D*-alaline (2.5 g, 28 mmol) was dissolved in ethanol (25 mL) and pyridine-4-carboxaldehyde (3.0056 g, 28 mmol) was dissolved in water (30 mL) which contained NaOH (1.12 g, 28 mmol). The two solutions was mixed and stirred at room temperature for 45 minutes before ice bath. Then aqueous solution (15 mL) of  $\text{NaBH}_4$  (1.27 g , 33.6 mmol) and NaOH (0.44 g , 11 mmol) was added and kept stirred for 30 minutes in ice bath. The solution was acidified with concentrated HCl to pH = 4. After reaction, the solvent was removed by rotary evaporation. The obtained white powder was purified by EtOAc and EtOH separately to give white product of *D*-HLN, yield of about 90%.

L-HLN was synthesized by the same method that mentioned above only by replacing *D*-alaline to L-alaline.

For L-HLN:  $^1\text{H NMR}$  (DMSO): 1.050 (s, 1H), 1.550 (t, 3H), 3.986 (s, 1H), 4.215 (s, 1H), 7.648(b, 2H), 8.646(b, 2H);  $^{13}\text{C NMR}$  (DMSO): 15.054, 55.120, 125.183, 141.922, 149.991, 171.235.

For *D*-HLN:  $^1\text{H NMR}$  (DMSO): 1.038 (s, 1H), 1.564 (t, 3H), 4.041 (s, 1H), 4.286 (s, 1H), 7.834 (b, 2H), 8.742 (b, 2H).  $^{13}\text{C NMR}$  (DMSO): 14.950, 55.096, 126.001, 142.167, 147.776, 171.094.

### Synthesis of D-NTU-18

A solution of Zn(OAc)·(H<sub>2</sub>O)<sub>2</sub> (60 mg, 0.273 mmol), *D*-HLN (20 mg, 0.091 mmol) and DMF (1.5 mL) was heated in a sealed vial (20 mL) at 80 °C for 48 h. After cooling to the room temperature, the colorless bulk-shaped crystals were obtained with high yield.

### Synthesis of L-NTU-18

A solution of Zn(OAc)·(H<sub>2</sub>O)<sub>2</sub> (60 mg, 0.273 mmol), *L*-HLN (20 mg, 0.091 mmol) and DMF (1.5 mL) was heated in a sealed vial (20 mL) at 80 °C for 72 h. After cooling to the room temperature, the colorless bulk-shaped crystals were obtained with high yield.

### Crystallographic Analyses

Single-crystal X-ray diffraction data were measured on a Bruker Smart Apex CCD diffractometer at 293 K using graphite monochromated Mo/K $\alpha$  radiation ( $\lambda = 0.71073 \text{ \AA}$ ). Data reduction was made with the Bruker Saint program. The structures were solved by direct methods and refined with full-matrix least squares technique using the SHELXTL package.<sup>1</sup> Non-hydrogen atoms were refined with anisotropic displacement parameters during the final cycles. Organic hydrogen atoms were placed in calculated positions with isotropic displacement parameters set to  $1.2 \times U_{eq}$  of the attached atom. The hydrogen atoms of the ligand and water molecules could not be located, but are included in the formula. The unit cell includes a large region of disordered solvent molecules, which could not be modeled as discrete atomic sites. We employed PLATON/SQUEEZE<sup>2,3</sup> to calculate the diffraction contribution of the solvent molecules and, thereby, to produce a set of solvent-free diffraction intensities; structures were then refined again using the data generated. CCDC 1520353-1520354 contains the supplementary crystallographic data for this paper. These data can be obtained free of charge from The Cambridge Crystallographic Data Centre via [www.ccdc.cam.ac.uk/data\\_request/cif](http://www.ccdc.cam.ac.uk/data_request/cif). Crystal data are summarized in Table S1.

**Table S1.** Crystal data and structure refinement of **L-NTU-18** and **D-NTU-18**

	<b>L-NTU-18</b>	<b>D-NTU-18</b>
Empirical formula	C <sub>11</sub> H <sub>14</sub> N <sub>2</sub> O <sub>4</sub> Zn	C <sub>11</sub> H <sub>14</sub> N <sub>2</sub> O <sub>4</sub> Zn
Formula weight	303.63	303.63
Crystal system	Tetragonal	Tetragonal
Space group	<i>P4</i> <sub>1</sub>	<i>P4</i> <sub>3</sub>
Unit cell dimensions	<i>a</i> = 12.800(3) Å <i>c</i> = 9.984(5) Å	<i>a</i> = 12.783(5) Å <i>c</i> = 9.966(7) Å
Volume	1635.8 (11) Å <sup>3</sup>	1628.5(17) Å <sup>3</sup>
Z	4	4
Density (calculated)	1.233 g/cm <sup>3</sup>	1.234 g/cm <sup>3</sup>
Mu(MoKa)	1.507 mm <sup>-1</sup>	1.514 mm <sup>-1</sup>
<i>F</i> <sub>(000)</sub>	624	620
Index ranges	-15 ≤ <i>h</i> ≤ 15 -15 ≤ <i>k</i> ≤ 15 -11 ≤ <i>l</i> ≤ 11	-15 ≤ <i>h</i> ≤ 11 -15 ≤ <i>k</i> ≤ 15 -11 ≤ <i>l</i> ≤ 11
Tot., Uniq. Data, R(int)	11714, 2963, 0.064	11080, 2852, 0.041
Observed data [ <i>I</i> > 2σ( <i>I</i> )]	2414	2463
Nref, Npar	2963, 165	2852, 165
R <sub>1</sub> , wR <sub>2</sub> , S	0.0529, 0.1348, 1.00	0.0490, 0.1382, 1.09
Flack	0.023(17)	0.052(12)
Max Shift	0	0

$$R = \frac{\sum ||F_o| - |F_c||}{\sum |F_o|}, \quad wR = \left\{ \frac{\sum [w(|F_o|^2 - |F_c|^2)^2]}{\sum [w(|F_o|^4)]} \right\}^{1/2} \quad \text{and} \quad w = \frac{1}{[\sigma^2(F_o^2) + (0.1452P)^2]} \quad \text{where} \quad P = \frac{(F_o^2 + 2F_c^2)}{3}$$

Table S2 Hydrogen Bonds for **L-NTU-18**.

D—H···A	<i>d</i> (H..A) (Å)	<i>d</i> (D..A) (Å)	Angle of D—H..A (°)
N2--H2D···O1	2.2	2.93(9)	139
C2--H2···O3	2.56	3.28(14)	135
C5--H5···O1	2.53	3.12(12)	122
C5--H5···O4	2.41	3.26(17)	154
C8--H8B···O2	2.59	2.94(15)	102
C8--H8C···O4	2.55	3.41(18)	151

Table S3 Hydrogen Bonds for **D-NTU-18**.

D—H···A	<i>d</i> (H..A) (Å)	<i>d</i> (D..A) (Å)	Angle of D—H..A (°)
N2--H2C···O2	2.01	2.84(4)	142
C2--H2A···O2	2.57	3.42(3)	153
C1—H1A···O1	2.57	3.04(3)	113
C2—H2A···O3	2.53	3.22(3)	132
C5—H5A···O4	2.33	3.15(3)	148
C5—H5A···O2	2.38	2.96(2)	120

## Structural information

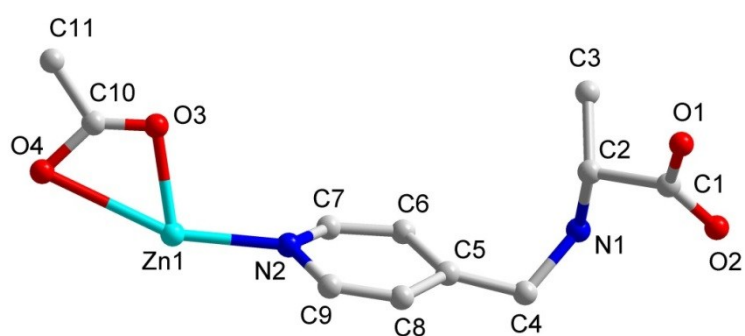


**Figure S1** Asymmetric unit of *D*-NTU-18.

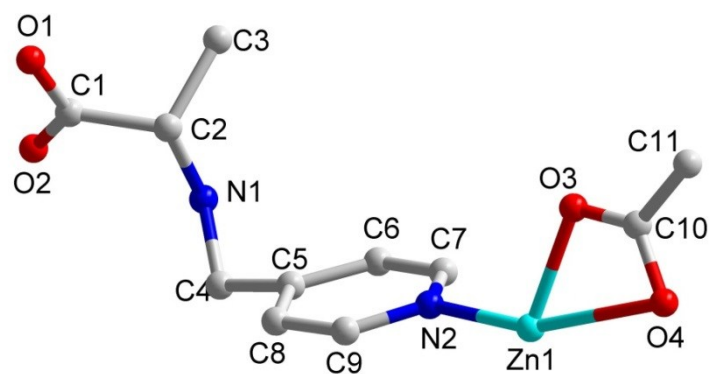


**Figure S2** Asymmetric unit of *L*-NTU-18.

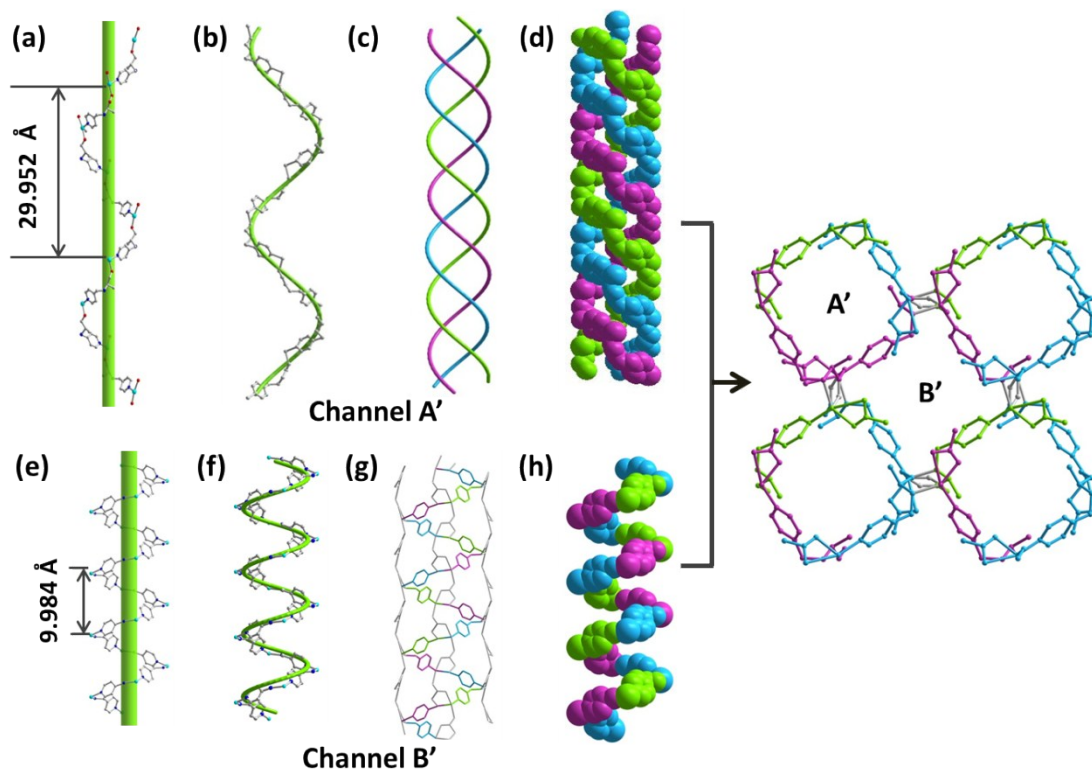


**Figure S3.** The  $4_1$  screw axis helical chain with longer pitch in channel A' (a and b); the simplification and space-filling of twisted three equal helix chains along  $b$ -axis in channel A' (c and d); the  $4_1$  screw axis helix chain with shorter pitch in channel B' (e and f); the connection of adjacent ligands in channel B' (g); the space-filling of the single helical chain along  $b$ -axis in channel B' (h); packing view of L-NTU-18 along  $c$ -axis.

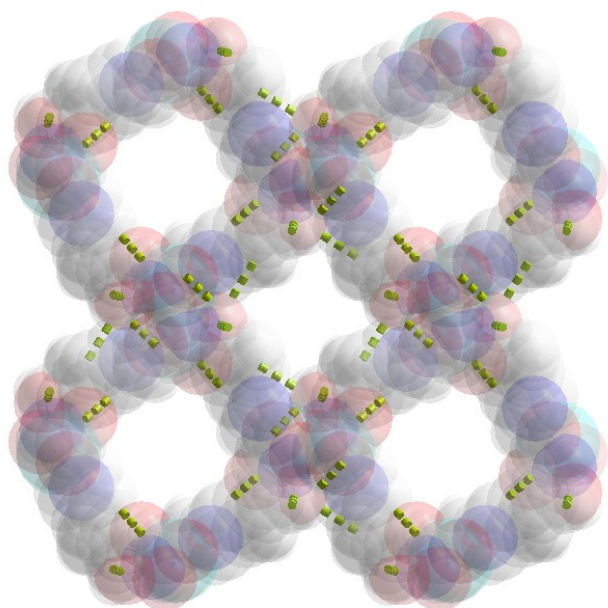


**Figure S4** Packing view of space filling and involved hydrogen bonds of *L*-NTU-18.

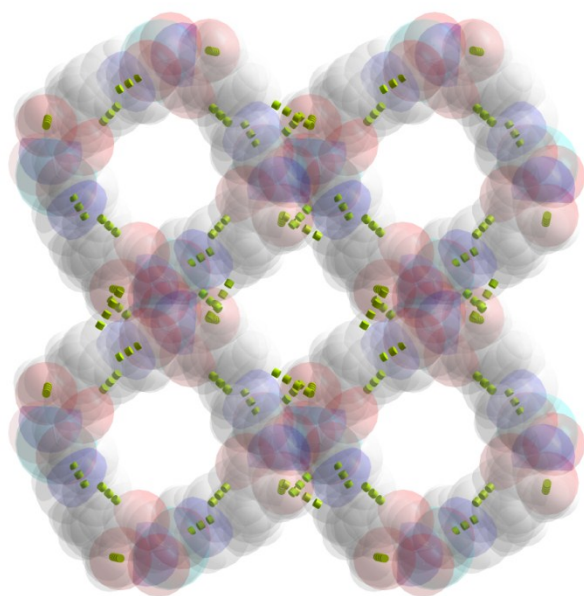


**Figure S5** Packing view of space filling and involved hydrogen bonds of *D*-NTU-18.

## Structural characterization

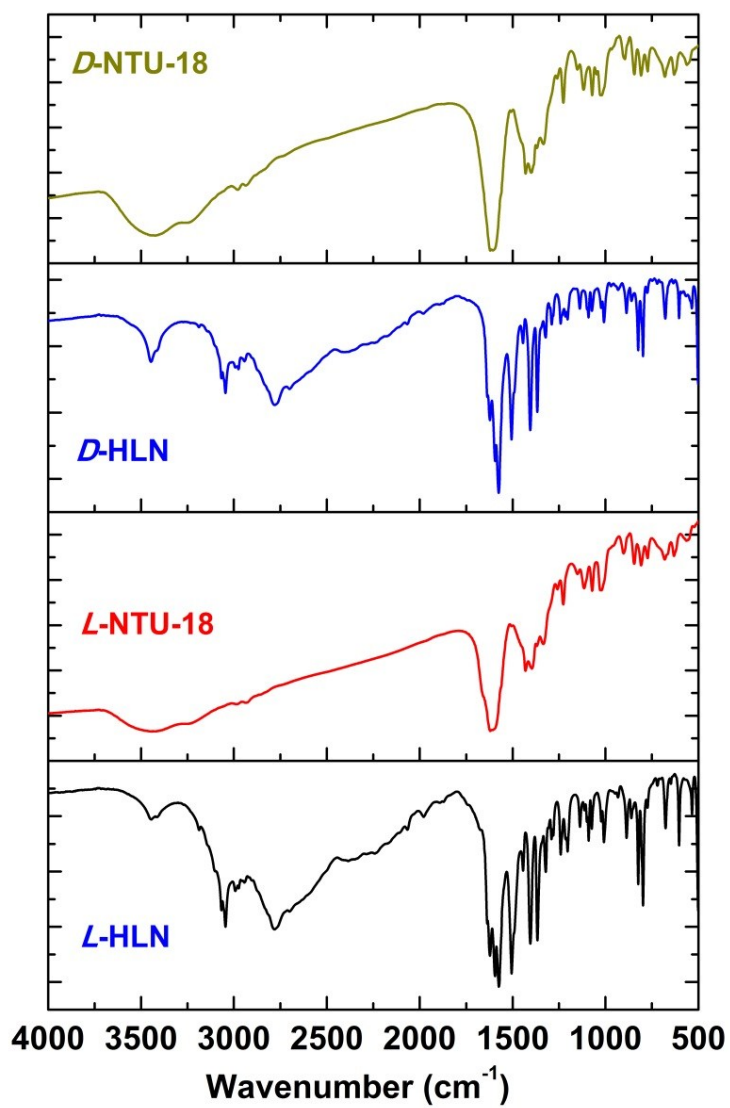


Figure S6 IR of involved ligands and as-synthesized *L*-NTU-18 and *D*-NTU-18.

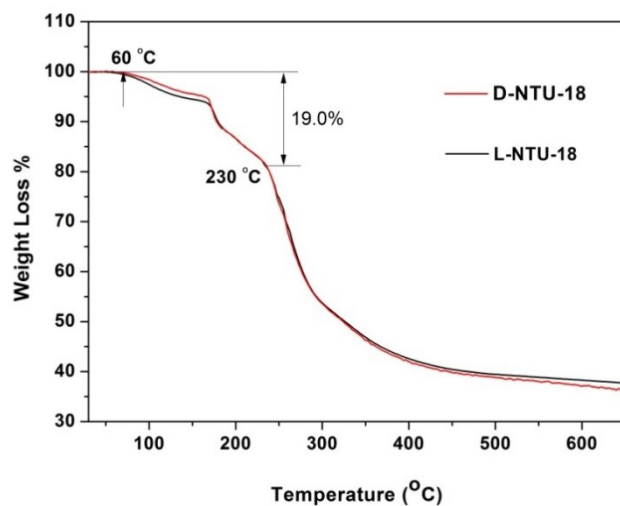


Figure S7 TG of as-synthesized **D-NTU-18** and **L-NTU-18**.

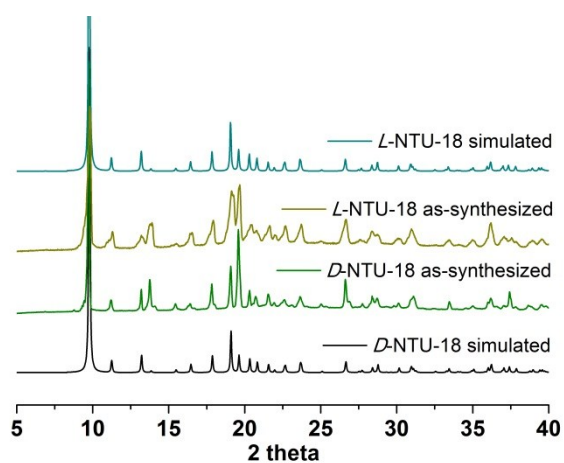


Figure S8 PXRD of simulated and as-synthesized **D-NTU-18** and **L-NTU-18**.

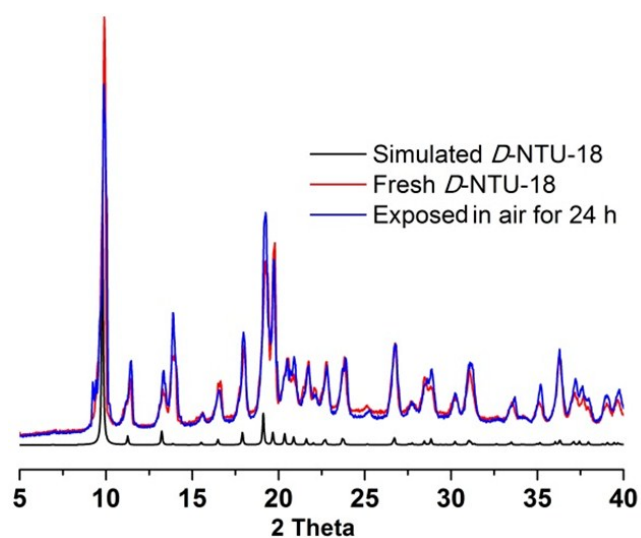
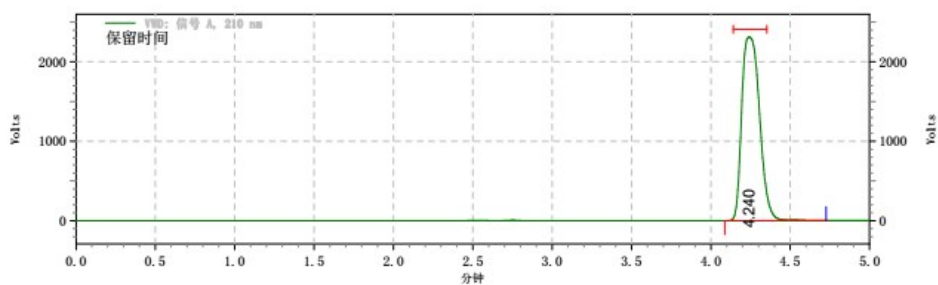


Figure S9 PXRD of **D-NTU-18** (exposed in air for 24h).

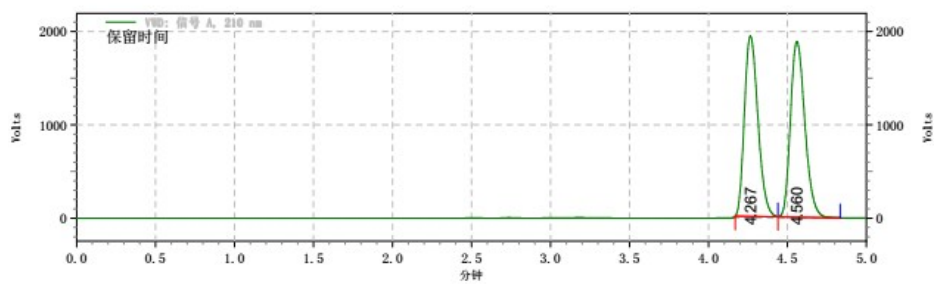
### **Separation process and characterization**

The hexane exchanged and dried **D-NTU-18** (~40 mg) was immersed in racemic 1-phenyl-1-propanol with varied concentration and temperature for 48 h, then, filtered, and washed crystal surface thoroughly with hexane. The absorbed guests were exchanged out by soaking the inclusion crystals in ethanol, respectively. Then, the contents of the enantiomers were analyzed by chiral high-performance liquid chromatography (HPLC) system (Agilent 1200 Series) equipped with a diode array detector (DAD) and an autosampler. Chromatographic separations were performed at 30°C using a CHIRALPAK OD-H column (5 µm, 4.6 mm × 250 mm). The analyses were performed by a UV detector at 210 nm using a mobile phase consisting of 85% *n*-Hexane, 15% isopropyl alcohol at a flow rate of 1.1 mL·min<sup>-1</sup>. The injected sample volume was 2 µL. The enantiomeric excess (*e.e.*) was determined from the peak areas of their two enantiomers, *S*-isomer and *R*-isomer.



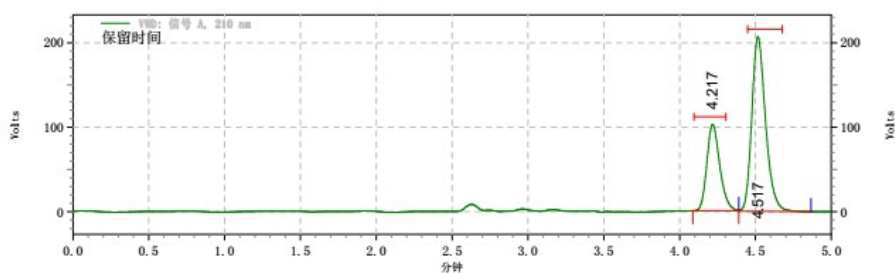
	Retention time	Area %
<i>R</i>	4.240	100
total		100

**Figure S10** HPLC graphs of racemic *R*-1-phenyl-1-propanol baseline.



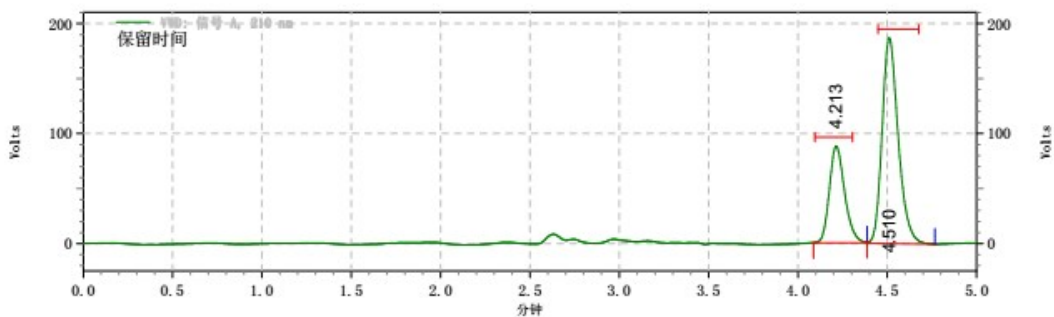
	Retention time	Area %
<i>R</i>	4.267	49.50
<i>S</i>	4.560	50.50
total		100

**Figure S11** HPLC graphs of racemic 1-phenyl-1-propanol baseline.



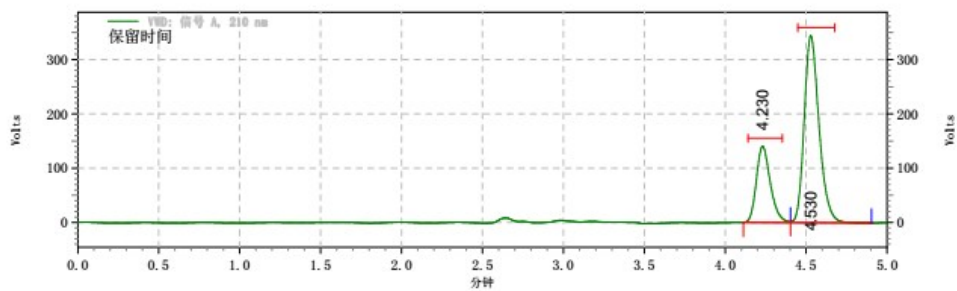
	Retention time	Area %
<i>R</i>	4.217	31.73
<i>S</i>	4.517	68.27
total		100
ee	36.54	

**Figure S12** HPLC graphs of entseparation of racemic 1-phenyl-1-propanol (50  $\mu$ L) at 3  $^{\circ}$ C.



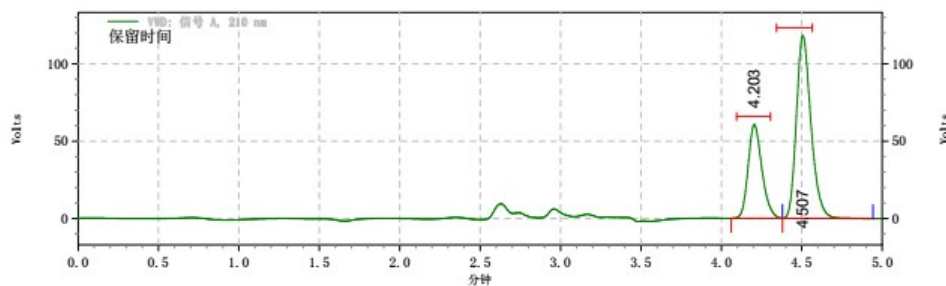
	Retention time	Area %
<i>R</i>	4.217	30.71
<i>S</i>	4.517	69.29
total		100
ee	38.58	

**Figure S13** HPLC graphs of entseparation of racemic 1-phenyl-1-propanol (150  $\mu$ L) at 3  $^{\circ}$ C.



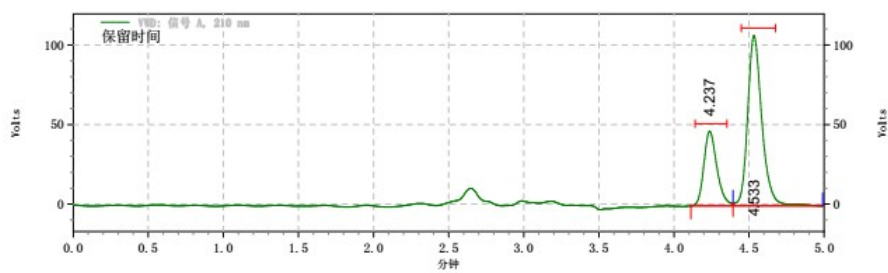
	Retention time	Area %
<i>R</i>	4.217	27.71
<i>S</i>	4.517	72.29
total		100
ee	44.58	

**Figure S14** HPLC graphs of entiseperation of racemic 1-phenyl-1-propanol (50  $\mu$ L) at 25  $^{\circ}$ C.



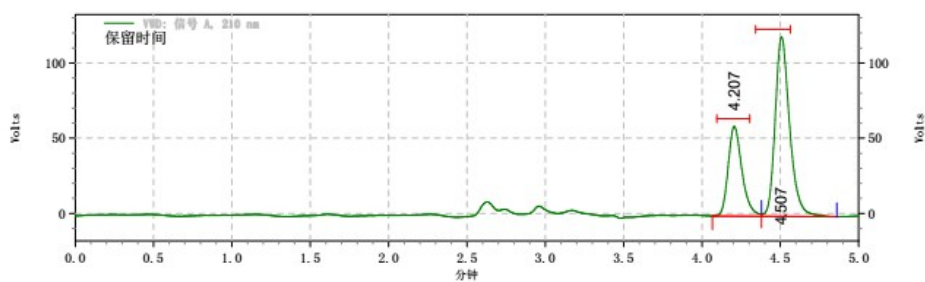
	Retention time	Area %
<i>R</i>	4.203	32.61
<i>S</i>	4.507	67.39
total		100
ee	34.78	

**Figure S15** HPLC graphs of entiseperation of racemic 1-phenyl-1-propanol (150  $\mu$ L, absorbed in hexane) at 3  $^{\circ}$ C.



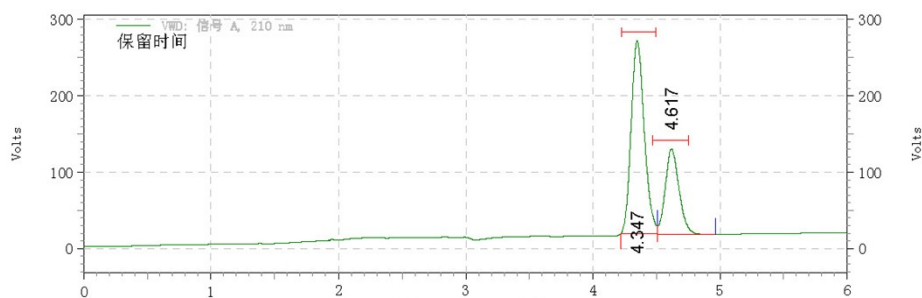
	Retention time	Area %
<i>R</i>	4.217	28.57
<i>S</i>	4.517	71.43
total		100
ee	42.86	

**Figure S16** HPLC graphs of entiseparation of racemic 1-phenyl-1-propanol (500  $\mu$ L, absorbed in hexane) at 3  $^{\circ}$ C.



	Retention time	Area %
<i>R</i>	4.207	32.22
<i>S</i>	4.507	67.78
total		100
ee	38.56	

**Figure S17** HPLC graphs of entiseparation of racemic 1-phenyl-1-propanol (1000  $\mu$ L, absorbed in hexane) at 3  $^{\circ}$ C.



	Retention time	Area %
R	4.347	68.42
S	4.617	31.58
total		100
ee	36.84	

**Figure S18** HPLC graphs of entiseparation of racemic 1-phenyl-1-propanol (50  $\mu$ L) by *L*-NTU-18 at 25  $^{\circ}$ C.

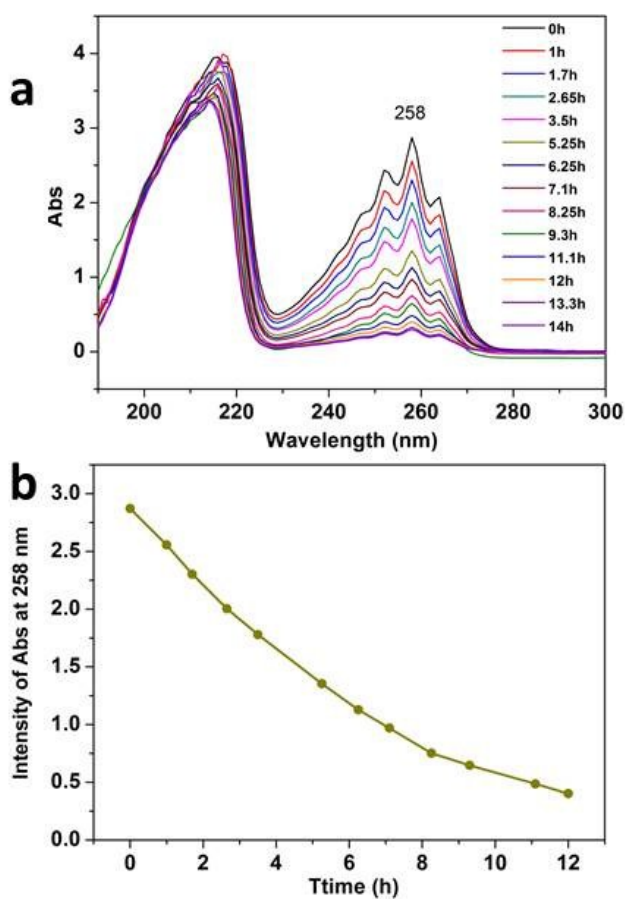


**Figure S19** UV spectra of racemic 1-phenyl-1-propanol (3 $\mu$ L) that adsorbed by *D*-NTU-18 ( $\sim$ 40 mg) in hexane (3 mL) (a); the time course of adsorbed 1-phenyl-1-propanol that generated from the peak intensity at 258 nm.

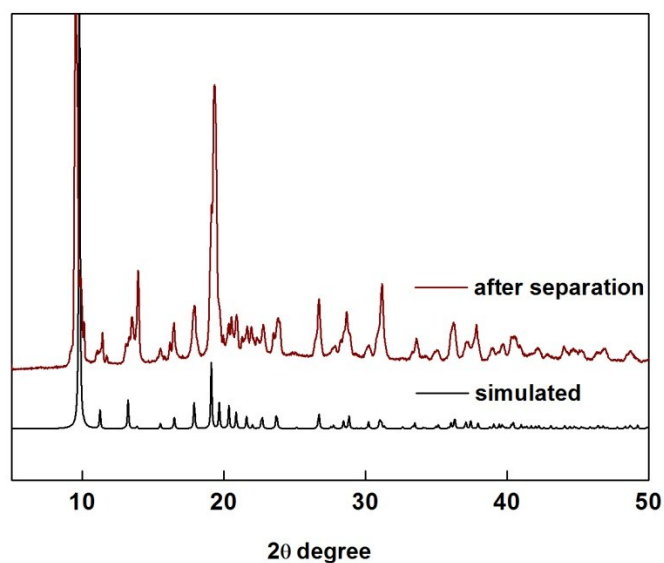


**Figure S20** PXRD pattern showed that **D-NTU-18** could keep its original phase after one round adsorption and guest releasing.

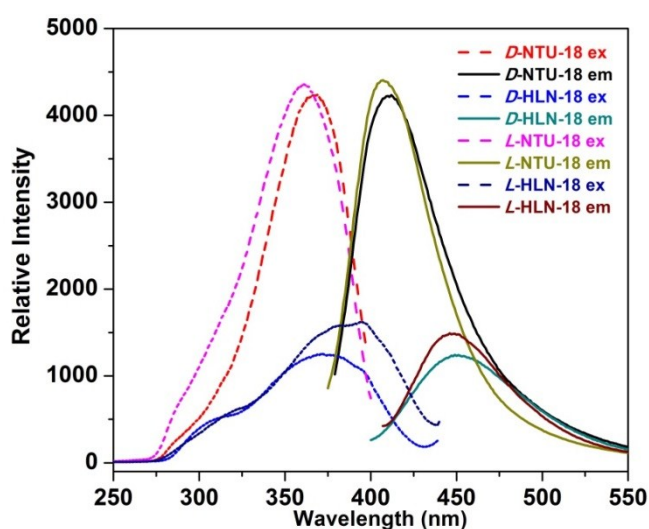


**Figure S21** Luminescent spectra of solid **D-NTU-18** and **L-NTU-18** at room temperature. The solid-state luminescence of those two PCPs showed maxima peaks at 410 nm ( $\lambda_{\text{ex}} = 360$  nm) and 405 nm ( $\lambda_{\text{ex}} = 370$  nm) for **L-/D-NTU-18**, respectively. In contrast, the luminescence spectra of free ligands show maximum emission peak at  $\sim 450$  nm under excitation at  $\sim 380$  nm. Taking the stable  $d^{10}$  electron configuration of  $\text{Zn}^{2+}$  in mind, the shift maxima emission and enhanced luminescent intensity should be attributed to the increased “rigidity” of the ligands by coordination and thus reduces the loss of energy through a radiationless pathway<sup>4-6</sup>.

## References

- (1) Sheldrick, G. M. *Acta Crystallogr. Sec. A* **2008**, *64*, 112.
- (2) Vandersluis, P.; Spek, A. L. *Acta Crystallogr. Sec. A* **1990**, *46*, 194.
- (3) Spek, A. L. *J. Appl. Crystallogr.* **2003**, *36*, 7.
- (4) Duan, J. G.; Zheng, B. S.; Bai, J. F.; Zhang, Q. A.; Zuo, C. Y. *Inorg. Chim. Acta* **2010**, *363*, 3172.
- (5) Cui, Y. J.; Yue, Y. F.; Qian, G. D.; Chen, B. L. *Chem. Rev.* **2012**, *112*, 1126.
- (6) Allendorf, M. D.; Bauer, C. A.; Bhakta, R. K.; Houk, R. J. T. *Chem. Soc. Rev.* **2009**, *38*, 1330.